

- A. Sperduto, Phys. Rev. **138**, B597 (1965).
- ⁸P. Wilhelm, O. Hansen, J. R. Comfort, C. K. Bockelman, P. D. Barnes, and A. Sperduto, Phys. Rev. **166**, 1121 (1968).
- ⁹W. E. Dorenbusch, O. Hansen, D. J. Pullen, T. A. Belote, and G. Sidenius, Nucl. Phys. **81**, 390 (1966).
- ¹⁰S. Hinds and R. Middleton, Nucl. Phys. **A92**, 422 (1967).
- ¹¹A. M. Bernstein, E. P. Lippincott, G. T. Sample, and C. B. Thorn, Nucl. Phys. **A115**, 79 (1968).
- ¹²K. Matsuda, Nucl. Phys. **33**, 536 (1962).
- ¹³T. A. Belote, W. E. Dorenbusch, O. Hansen, and A. Sperduto, Phys. Letters **14**, 323 (1965).
- ¹⁴S. M. Matin, D. J. Church, and G. E. Mitchell, Phys. Rev. **150**, 906 (1966).
- ¹⁵D. J. Church, R. N. Horoshko, and G. E. Mitchell, Phys. Rev. **160**, 894 (1967).
- ¹⁶C. D. Kavaloski and W. J. Kossler, Phys. Rev. **180**, 971 (1969).
- ¹⁷C. F. Monahan, I. G. Main, F. M. Nicholas, M. F. Thomas, and P. J. Twin, Nucl. Phys. **A130**, 209 (1969).
- ¹⁸B. van Nooljen, P. Mostert, J. F. van der Brugge, and A. H. Wapstra, Physica **23**, 753 (1957).
- ¹⁹E. C. Booth, B. Chasan, and K. A. Wright, Nucl. Phys. **57**, 403 (1964).
- ²⁰N. V. DeCastro Faria, J. Charbonneau, J. L'Ecuyer, and R. J. A. Levesque, Nucl. Phys. **A174**, 37 (1971);
- O. Häusser, D. Pelte, T. K. Alexander, and H. C. Evans, *ibid.* **A150**, 417 (1970).
- ²¹J. B. Marion, Nucl. Data **A4**, 301 (1968).
- ²²T. T. Bardin, J. A. Becker, T. R. Fisher, and A. D. W. Jones, Phys. Rev. C **4**, 1625 (1971).
- ²³E. K. Warburton, D. E. Alburger, and D. H. Wilkinson, Phys. Rev. **129**, 2180 (1963).
- ²⁴P. Paul, J. B. Thomas, and S. S. Hanna, Phys. Rev. **147**, 774 (1966).
- ²⁵E. K. Warburton, J. W. Olness, and A. R. Poletti, Phys. Rev. **160**, 938 (1967).
- ²⁶J. Lindhard, M. Scharff, and J. E. Schiøtt, Kgl. Danske Videnskab. Selskab Mat.-Fys. Medd. **33**, No. 14 (1963).
- ²⁷A. E. Blaugrund, Nucl. Phys. **88**, 501 (1966).
- ²⁸J. H. Ormrod, J. R. MacDonald, and H. E. Duckworth, Can. J. Phys. **43**, 275 (1965).
- ²⁹L. C. Northcliffe and R. F. Schilling, Nucl. Data **A7**, 233 (1970).
- ³⁰J. Vervier, Nucl. Phys. **A103**, 222 (1967).
- ³¹D. H. Wilkinson, Comments Nucl. Particle Phys. **1**, 139 (1967).
- ³²R. D. Lawson, private communication.
- ³³L. Zamick, Nucl. Phys. **A154**, 191 (1970).
- ³⁴M. Soga, R. N. Horoshko, and D. M. Van Patter, Phys. Letters **26B**, 727 (1968).

(p, t) and $(p, {}^3\text{He})$ Reactions on ^{27}Al at $E_p = 27$ MeV*

R. Graetzer,† J. J. Kraushaar, and J. R. Shepard

Nuclear Physics Laboratory, Department of Physics and Astrophysics,
University of Colorado, Boulder, Colorado 80302

(Received 25 August 1972)

Levels in ^{25}Al and ^{25}Mg were populated via the (p, t) and $(p, {}^3\text{He})$ reactions with 27-MeV protons on a ^{27}Al target. Angular distributions of emitted tritons and ${}^3\text{He}$ were measured simultaneously with a detector telescope. Zero-range distorted-wave Born-approximation (DWBA) calculations with simple shell-model configurations for the two transferred nucleons provided satisfactory fits for several of the observed diffraction patterns. A sharp rise in cross section at forward angles was a good indication of the presence of $L=0$ transfer even though transitions occurred with a mixture of L values. Compound-nucleus calculations reproduced the smooth angular-distribution shapes observed for higher excited levels but predicted cross sections consistently larger than those observed. For the first $\frac{1}{2}^{\pm}$ levels neither DWBA, compound-nucleus, nor a direct two-step (p, d) (d, t) calculation were able to give a satisfactory description of the data.

I. INTRODUCTION

The (p, t) reaction has been utilized with considerable success to determine energies, spins, and parities, and to check nuclear wave functions in even- A nuclei. In a recent study of the (p, t) reaction on even- A titanium isotopes Baer *et al.*^{1,2} carefully investigated the advantages as well as the limitations of the (p, t) reaction. However, use of the (p, t) reaction on odd- A targets for spectroscopic purposes has not been extensive.

One reason may be that the high level density in the residual odd- A nucleus requires relatively better energy resolution. Also the determination of the spins and parities of residual states from the triton angular distributions can be difficult because several L values may be mixed.

In order to assess the impact of L mixing and other complexities on the interpretation of the two-nucleon transfer reaction on odd- A target nuclei, we selected ^{27}Al as the target. The energies, spins, and parities of low excited states in

^{27}Al are well known³ and the level density is not too great for the energy resolution of our equipment.

Another reason for selecting ^{27}Al was that the $(p, ^3\text{He})$ reaction, which was studied simultaneously, leads to mirror levels in ^{25}Mg . Comparison of the two reactions is of interest because the isospin selection rules differ. The two neutrons picked up in the (p, t) reaction are assumed to be coupled to isospin $T=1$ and intrinsic spin $S=0$. The proton and neutron picked up in the $(p, ^3\text{He})$ reaction may be coupled to either $S=0$, $T=1$ or $S=1$, $T=0$ and thus permit a larger variety of transferred LSJ combinations. Ratios of (p, t) and $(p, ^3\text{He})$ cross sections have been used⁴ to identify $T=\frac{3}{2}$ analog states and, in restricted cases, to obtain information about their structure. However, these simple theoretical expressions for the cross-section ratios are not applicable here because the highest excitation energy studied here is 6 MeV which is below the lowest $T=\frac{3}{2}$ states.

Finally, there was considerable interest in obtaining information about the ground-state wave function of ^{27}Al about which there is a puzzling question. Both the weak-coupling (vibrational) model and the strong-coupling (rotational) model have been applied to ^{27}Al . Each model has had remarkable successes and notable failures which have been discussed in detail by Bohne *et al.*⁵

Data for the (p, t) and $(p, ^3\text{He})$ reactions on ^{27}Al leading to low excited states in ^{25}Al and ^{25}Mg have not been published previously apart from two preliminary oral reports.^{6,7} Hardy and co-workers^{8,9} studied both reactions but dealt only with transitions to the ground states and the lowest $T=\frac{3}{2}$ states which have excitation energies of about 8 MeV. Our experimental procedures and the data obtained are discussed briefly in Sec. II below. A distorted-wave Born-approximation (DWBA) analysis of the data is described in Sec. III. Computations of cross sections for populating levels in ^{25}Al and ^{25}Mg via compound-nucleus formation are also included in Sec. III. Some preliminary coupled-channels calculations of two-step contributions to the reaction cross section are presented in the same section. Our conclusions are presented in the final section. Some preliminary results of this experiment have already been reported.¹⁰

II. EXPERIMENTAL PROCEDURES AND RESULTS

A beam of 27-MeV protons, obtained from the University of Colorado azimuthally varying field cyclotron, was focused onto an Al foil (0.42 mg/cm²) at the center of a 91-cm-diam scattering chamber. The foil was prepared by

rolling Al initially in a sandwich of chromium-plated steel and finally in a sandwich of stainless steel. The foil thickness was determined both by weighing and by measuring the energy lost in the foil by 5.5-MeV α particles from a ^{241}Am source. The scattering chamber was equipped with two rotatable cooled holders for solid-state charged-particle detectors. A 5–6-mm-thick Si(Li) detector positioned at a laboratory scattering angle of 90° was used as a beam and target monitor. A three-detector telescope, used for detection and mass identification of reaction products, consisted of a 43- μm ΔE surface-barrier detector, a 500- μm E surface-barrier detector, and a 5–6-mm-thick Si(Li) veto detector. The veto detector served to reduce the number of events processed by the particle identification electronics and thus permitted use of beam currents up to 1 μA . Additional details about the equipment, electronics for mass identification, and data storage and handling are given in Ref. 2.

Triton and ^3He spectra were obtained at a laboratory scattering angle of 7.5° and at angles from 10 to 120° in 5° increments. The Q values for the $^{27}\text{Al}(p, t)$ and $(p, ^3\text{He})$ reactions are -15.93 and -11.65 MeV, respectively, computed from the 1971 mass excess tables.¹¹ Thus the outgoing triton and ^3He energies range downward from 11.1 and 15.4 MeV, respectively. The observed energy resolution in the triton spectra ranged from 70 to 120 keV full width at half maximum (FWHM) depending on the effective target thickness for the outgoing particles and on the angular acceptance of the detector. The FWHM in the ^3He spectra ranged up to 150 keV. Spectra obtained at 30° are shown in Fig. 1. The similarity of the peak positions (energies) and relative intensities of groups in the mirror nuclei ^{25}Al and ^{25}Mg is striking. The energies of the triton and ^3He groups were determined from a linear energy calibration based on the ground states and the prominent 1.61-MeV levels. For levels to 3.4 MeV in ^{25}Mg and to 4 MeV in ^{25}Al our energies are in excellent agreement (± 25 keV) with energies previously determined.¹² At excitation energies above 4 MeV in ^{25}Mg the level density prohibits unique level identification. In ^{25}Al we also observed groups for which the kinematic shift with angle is consistent with assignment of previously unreported levels at 4.67, 5.60, and 5.90 MeV. The 4.59 + 4.67-MeV peak in the triton spectrum (FWHM = 160 keV) appeared as a broad unresolved multiplet in all of our spectra. If the target contained oxygen, a peak corresponding to the ground-state transition for $^{16}\text{O}(p, t)^{14}\text{O}$ should have moved through the 4.59 + 4.67-MeV group with increasing scattering angle. However, there was no evidence for the

existence of this ${}^{14}\text{O}$ peak at forward scattering angles where it should be well separated from ${}^{25}\text{Al}$ groups and have its greatest intensity.¹³ The three new levels reported here were not observed in a current ${}^{24}\text{Mg}({}^3\text{He}, d){}^{25}\text{Al}$ experiment.¹⁴ However, a level at 5.578 MeV was observed¹⁵ in the reaction ${}^{24}\text{Mg}(p, p'\gamma)$.

The experimental differential cross sections as a function of scattering angle are presented graphically in Figs. 2-4. The error bars indicate only the uncertainties in the Gaussian fitting and background subtraction computed with the code SPECTR.¹⁶ Uncertainties in resolving doublets vary considerably and have not been included. Uncertainties in target orientation and detector position should make only very small contributions to the over-all uncertainty. The largest

systematic uncertainties include those in target thickness (8%), detector solid angle (3%), and current integration (1%). Cross sections determined for the stronger well-resolved levels were reproducible to within 15%.

III. DISTORTED-WAVE AND COMPOUND-NUCLEUS ANALYSES

A. Basic Description of DWBA

Analysis of direct two-nucleon transfer reactions has usually been carried out in terms of the DWBA theory with a zero-range interaction as described by Glendenning¹⁷ and by Towner and Hardy.⁹ Derivation of expressions relevant to the widely used computer code DWUCK¹⁸ appeared as an Appendix in Ref. 2. The differential cross sec-

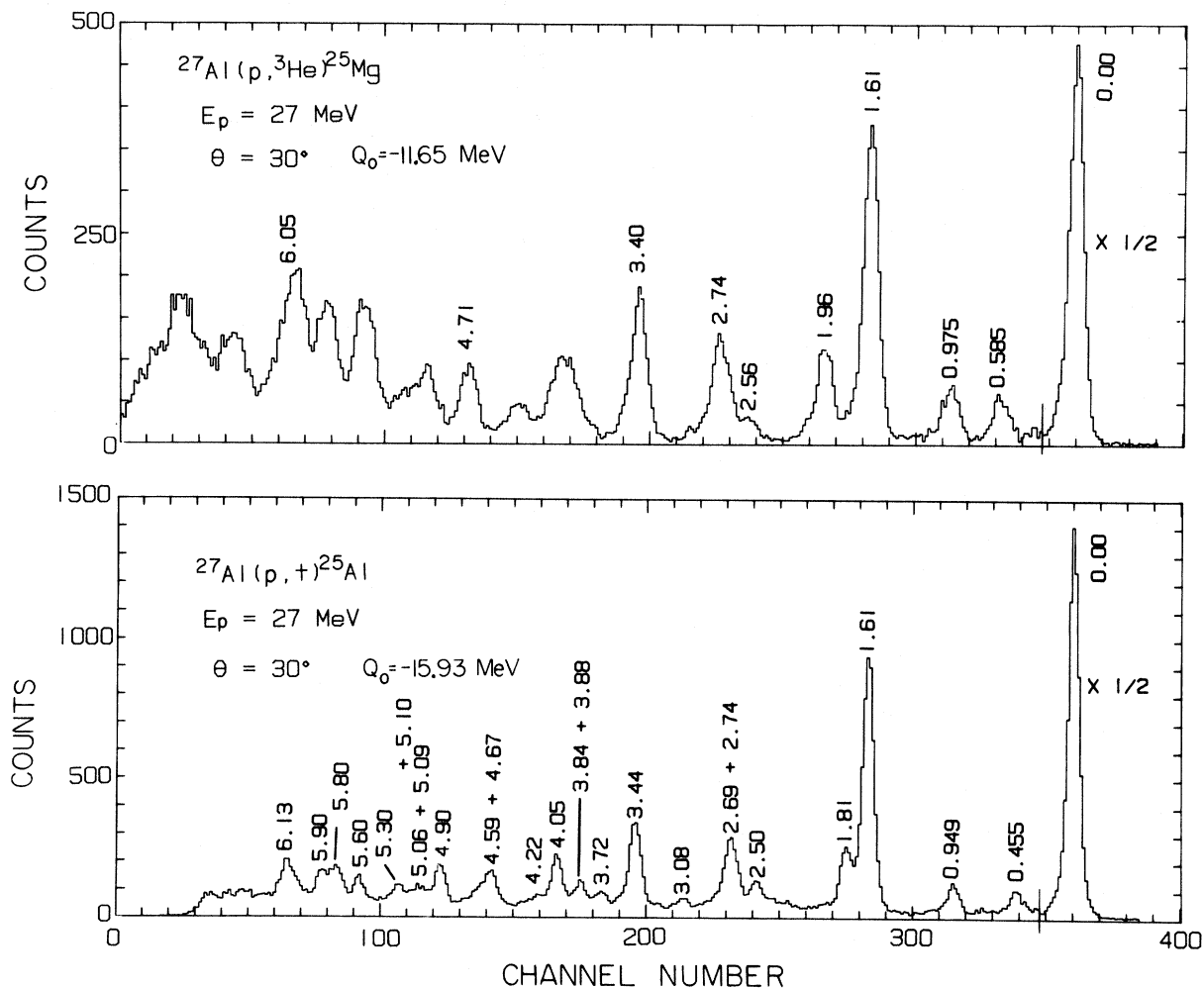


FIG. 1. Spectra of ${}^3\text{He}$ particles and triton emitted at a laboratory scattering angle of 30° during bombardment of ${}^{27}\text{Al}$ with 27-MeV protons. A total charge of $390 \mu\text{C}$ was collected. The FWHM for the ${}^3\text{He}$ spectrum is about 140 keV and for the triton spectrum, about 110 keV. The assigned energies are taken from Ref. 12. New Levels in ${}^{25}\text{Al}$ are tentatively proposed at 4.67, 5.60, and 5.90 MeV.

tion for the direct two-nucleon pickup reaction can be obtained from Eqs. (A9), (A10), (A11), and (A21) of Ref. 2. The required distorted waves are derived from an optical-model potential discussed in Sec. IIIB. The selection of shell-model configurations for the transferred nucleons is discussed in detail in Sec. IIIC.

B. Optical-Model Parameters

The distorted waves describing the incident proton and emitted ^3He or triton are obtained by solving the Schrödinger equation with a complex potential well. Optical-model potentials which successfully describe elastic scattering are usually

employed. The proton potential and values for the relevant parameters listed in Table I were obtained by Satchler from his analysis¹⁹ of elastic scattering of 30-MeV protons from ^{28}Si . These parameter values are not expected to be very sensitive to proton energy or target mass and therefore should be satisfactory for describing 27-MeV protons incident on ^{27}Al .

Potentials for ^3He and triton scattering differ only by a small isospin term²⁰ which was neglected in our computations. Seven different sets of parameter values for mass-3 projectiles are listed in Table I. The sets labeled ZF, M, and GJ were obtained from the references²¹⁻²³ cited in the table. The set GJ resulted from a three-parameter (V, a, W) search in which $a' = a$ and $R' = R = 1.3$ fm. We made two five-parameter searches, denoted GJS and GJD, with $R = 1.14$ fm on the data (up to 140°) used to determine set GJ. The search for the set GJS was started with a shallow real well ($V = 135$ MeV) while the search leading to the set GJD was begun with a deep real well ($V = 175$ MeV). The sets GJS and GJD did not give significantly better fits to the elastic scattering data. The Coulomb radius R_c was fixed at 1.4 fm for these two searches. Two more searches with $R_c = 1.25$ fm yielded almost the same parameter values for the shallow well but generated quite different values for the deep well. The quality of the fit for the deep well, as measured by χ^2 , was not

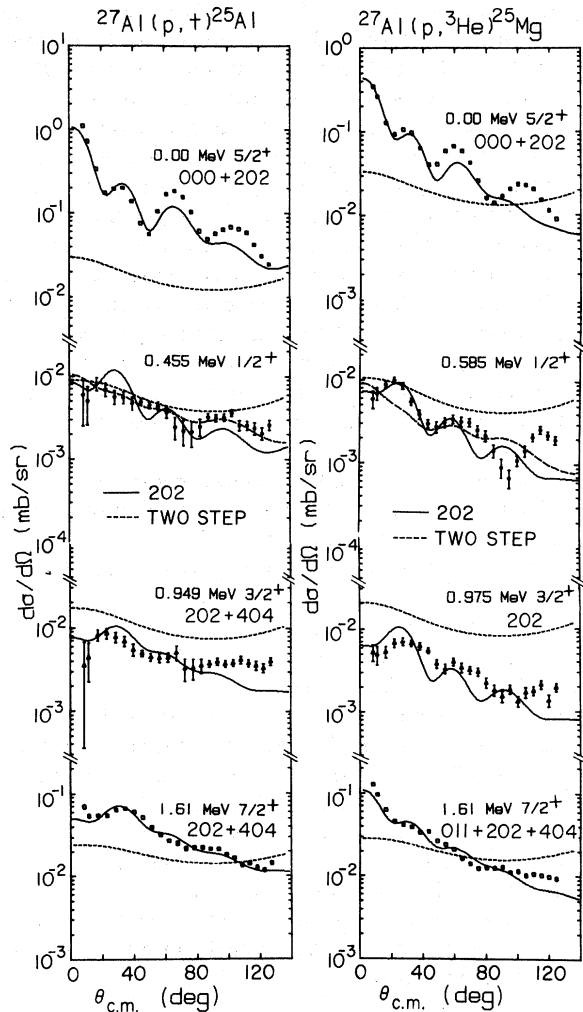


FIG. 2. Triton and ^3He angular distributions for mirror levels in ^{25}Al and ^{25}Mg up to 1.61 MeV excitation. The theoretical predictions are discussed in Sec. IIID and E. The DWBA predictions are labeled with the transferred LSJ values. The dashed curves are the compound-nucleus cross sections.

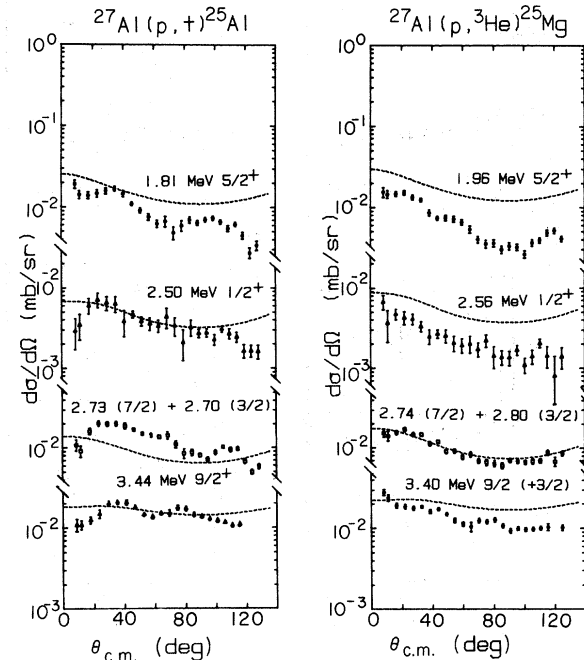


FIG. 3. Experimental triton and ^3He angular distributions for mirror levels in ^{25}Al and ^{25}Mg between 1.81 and 3.5 MeV excitation.

so good as that obtained with $R_c = 1.4$ fm.

The set C,²⁴ characterized by a deep well and volume absorption, is based on elastic scattering of 20-MeV tritons and 21-MeV ${}^3\text{He}$ from ${}^{40}\text{Ca}$, ${}^{52}\text{Cr}$, ${}^{54}\text{Cr}$, ${}^{54}\text{Fe}$, ${}^{62}\text{Ni}$, ${}^{64}\text{Ni}$, ${}^{90}\text{Zr}$, ${}^{92}\text{Zr}$, and ${}^{94}\text{Zr}$. The energy-dependent set CR,²⁵ which has a shallow real well and strong surface absorption but no volume absorption was developed to describe ${}^3\text{He}$ elastic scattering from ${}^{40}\text{Ca}$ in the energy range 20–80 MeV. This set is almost equivalent to the set T6 used successfully by Baer *et al.*² for analysis of (p, t) data from titanium isotopes and by Shepard, Kraushaar, and Graetzer²⁶ for ${}^{48}\text{Cr}$ and ${}^{68}\text{Ge}$ data.

To determine whether sets C and CR were applicable to our experiment, we obtained predictions for elastic scattering of 15-MeV ${}^3\text{He}$ from ${}^{24}\text{Mg}$ and 12-MeV tritons from ${}^{27}\text{Al}$. The predictions are compared with experimental data in Figs. 5 and 6. It is apparent that the extrapolation of parameter sets C and CR to the lower bombarding energies and lighter mass targets is not completely satisfactory. The parameter set ZF was used for nearly all of our data analyses.

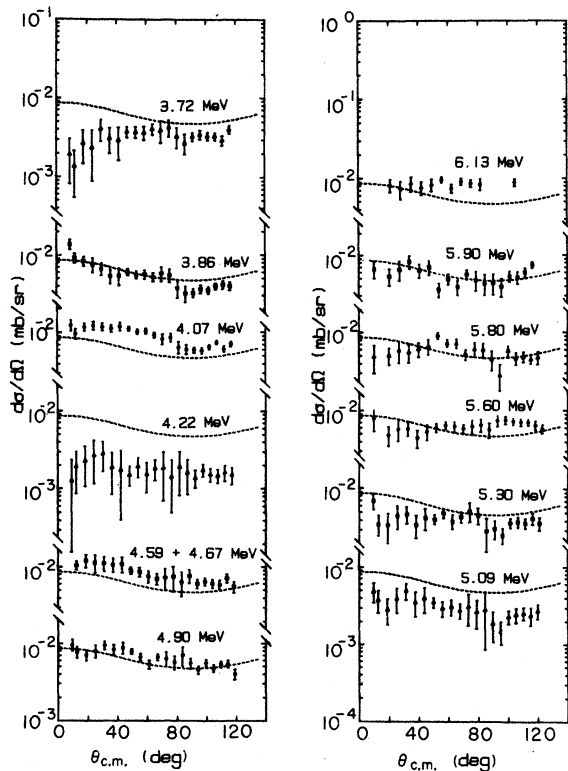


FIG. 4. Triton angular distributions for levels above 3.5 MeV excitation in ${}^{25}\text{Al}$. A single compound-nucleus calculation for a level at 5 MeV with spin $\frac{5}{2}$ is shown (dashed line) with each experimental angular distribution.

C. Bound-State Orbits

The simplest shell-model configuration for the target nucleus ${}^{27}\text{Al}$ consists of an inert ${}^{16}\text{O}$ core, six neutrons which fill the $d_{5/2}$ orbit, and five protons in the $d_{5/2}$ orbit. In other seniority-one configurations pairs of neutrons may be present in the $2s_{1/2}$ and/or $1d_{3/2}$ orbits. More complex configurations (seniority three) could involve two unpaired neutrons in any of the three s - d shell orbits. The lowest configurations that could lead to odd-parity states in ${}^{25}\text{Mg}$ or ${}^{25}\text{Al}$ would require pickup from the $1f_{7/2}$ orbit.

Because nuclear properties in the mass region near $A = 25$ have been interpreted in terms of the collective rotational model, we carried out some calculations with simple collective wave functions for which shell-model amplitudes have been given by Chi.²⁷ In the Nilsson representation²⁸ the $K = \frac{5}{2}$ ground state is a pure $d_{5/2}$ state because the $2s_{1/2}$ and $1d_{3/2}$ states cannot have angular momentum projections of $\frac{5}{2}$ along the nuclear symmetry axis. Because ${}^{27}\text{Al}$ may be in a transition region, band mixing has been employed to fit experimental $E2$ transition rates and inelastic scattering cross sections.²⁹ Many-particle shell-model wave functions for ${}^{27}\text{Al}$ have been generated by De Voigt *et al.*³⁰ but such wave functions are not yet available for mass 25. The distorted-wave computations discussed in Sec. III D are therefore restricted to simple configurations which are expected to be prominent.

Sensitivity of DWBA computations to the choice of neutron shell-model configurations was investigated for several transitions. As indicated in Fig. 7 there is virtually no dependence on the choice of configuration.

The potential and parameter values used for computation of the bound-state orbits are given in Table I. Although Baer *et al.*² found little sensitivity of DWBA calculations to the choice of the bound-state well radius R , we observed appreciable sensitivity as illustrated in Fig. 8 for both $L = 0$ and $L = 2$ transfer. The relative magnitudes of successive diffraction maxima and minima were altered considerably by a 9% increase in R . The smaller value of R was chosen for the computations discussed below because the predicted angular distributions for the ground-state transitions more nearly agreed with the data.

D. Distorted-Wave Analysis of Experimental Results

The low-lying excited levels in ${}^{25}\text{Al}$ and ${}^{25}\text{Mg}$, which have been interpreted³ as collective rotational bands of deformed nuclei, are shown in Fig. 9. The experimental angular distributions of tritons

and ${}^3\text{He}$ which leave the residual nuclei in the $J^\pi = \frac{5}{2}^+$ ground states are shown in Fig. 2. For the (p, t) reaction (with $S=0$) the transferred LSJ values permitted by conservation laws are 000, 202, and 404. Computations with DWUCK for two-neutron pickup from $(d_{5/2})^2$, $(s_{1/2})^2$, and $(d_{3/2})^2$ shell-model orbits were made with the triton-optical-model-parameter sets listed in Table I. For many cases two different radii for the neutron well, already discussed in Sec. III C, were used. The excellent fit shown in Fig. 2 was obtained with the ZF optical-model parameter values for a sum (incoherent) of 000 and 202 DWUCK cross sections with a $(d_{5/2})^2$ configuration and a neutron well radius of 1.15 fm. The sum of DWUCK cross sections was then scaled to provide the best fit to the data. Although a better fit could be obtained by weighting the 000 and 202 cross sections unequally, such a

procedure is probably not meaningful when only simple neutron configurations are employed. Moreover the equal weighting of the 000 and 202 components is appropriate for a filled $d_{5/2}$ sub-shell as DWUCK is presently programmed. It is clear from comparison of the data with the curves in Fig. 8 that both L values are required. Parameter value set M which is rather similar to ZF did not give as good a fit to the data. However, $(d_{3/2})^2$ pickup with $R=1.25$ fm yielded almost as satisfactory a fit as that illustrated.

For the $(p, {}^3\text{He})$ reaction to the ground state of ${}^{25}\text{Mg}$ LSJ transfers of 000, 202, 404 as well as 011, 211, 213, 413, 414, 415, and 615 are allowed but will be restricted if the two transferred nucleons are picked up from the same orbit.¹⁷ Once again the shape of the experimental angular distribution (Fig. 2) was reproduced quite well with

TABLE I. Optical and bound-state potential parameters: The optical-model potential

$$U(r) = -V(e^x + 1)^{-1} - i \left(W - 4W_D \frac{d}{dx'} \right) (e^{x'} + 1)^{-1} + \left(\frac{\hbar}{m_\pi c^2} \right) V_s \hat{\mathbf{I}} \cdot \hat{\mathbf{s}} r^{-1} \frac{d}{dr} (e^{x_s} + 1)^{-1} + V_C.$$

The bound-state potential

$$V(r) = V_b (e^x + 1)^{-1} + \left(\frac{\lambda}{45.2} \right) V_b \hat{\mathbf{I}} \cdot \hat{\mathbf{s}} r^{-1} \frac{d}{dr} (e^{x_s} + 1)^{-1} + V_C.$$

Here V_C is the Coulomb potential of a uniformly charged sphere of radius $R_c A^{1/3}$ and $x \equiv (r - RA^{1/3})/a$.

Identification	Experimental basis	V (MeV)	R (fm)	a (fm)	W (MeV)	W_D (MeV)	R' (fm)	a' (fm)	V_s (MeV)	R_s (fm)	a_s (fm)	R_c (fm)
Proton ^a	30-MeV p on ${}^{28}\text{Si}$	50.2	1.121	0.674	4.28	3.42	1.326	0.546	6.56	0.899	0.665	1.20
ZF ^b	15-MeV ${}^3\text{He}$ on ${}^{24}\text{Mg}$	164.0	1.14	0.69	14.7	...	1.60	1.08	1.4
M ^c	15-MeV ${}^3\text{He}$ on ${}^{30}\text{Si}$	173.0	1.07	0.795	18.6	...	1.657	0.762	1.4
GJ ^d	12-MeV t on ${}^{27}\text{Al}$	147.1	1.4	0.61	54.1	...	1.4	0.61	1.3
GJS ^e	12-MeV t on ${}^{27}\text{Al}$	141.4	1.14	0.723	48.86	...	1.374	0.716	1.4
GJD ^f	12-MeV t on ${}^{27}\text{Al}$	164.7	1.14	0.688	80.71	...	1.142	0.779	1.4
C ^g	20-MeV t and 21-MeV ${}^3\text{He}$ on $20 \leq Z \leq 40$	175.45	1.14	0.714	19.95	$\pm \epsilon W_1^h$	1.535	0.847	1.4
CR ⁱ	20-80-MeV ${}^3\text{He}$ on ${}^{40}\text{Ca}$	$\frac{137.6}{138.4}^i$	1.10	0.853	...	$\frac{20.85}{20.65}^i$	1.308	0.751	1.4
Bound state		V_b^j	1.15	0.65	$\lambda = 25$	1.25	0.65	1.25

^a Reference 19.

^b Reference 21.

^c Reference 22.

^d Based on a three-parameter (V, a, W) search. (Reference 23.)

^e Result of our search starting with a shallow $V=135$ MeV; R and R_c fixed.

^f Result of our search starting with a deep $V=175$ MeV; R and R_c fixed.

^g Reference 24.

^h The surface absorption term $W_D \equiv \pm \epsilon W_1$, where $\epsilon \equiv (N-Z)/A$, $W_1 = -9.32$ MeV, and the plus and minus signs are employed for ${}^3\text{He}$ and tritons, respectively.

ⁱ The energy dependence (Ref. 25) is given by $V = 141.6 - 0.27E$ and $W_D = 19.5 + 0.12E - 0.002E^2$, where E is the laboratory energy of the mass-3 particle. The upper number in the table refers to 15 MeV, the lower to 12-MeV particles.

^j The real well depth for the two neutrons was adjusted to give each orbit a binding energy of $0.5(S_{2n} + E_x)$ where S_{2n} is the two-neutron separation energy and E_x the excitation energy in the residual nucleus. For neutron plus proton pickup the proton well depth was the proton separation energy from ${}^{27}\text{Al}$ plus $0.5E_x$ while the neutron well depth was the neutron separation energy from ${}^{26}\text{Mg}$ plus $0.5E_x$.

the ZF parameters and proton-plus-neutron pick-up from the $(\pi d_{5/2}, \nu d_{5/2})$ orbits with a sum of 000 and 202 DWUCK cross sections. Note that the $(p, {}^3\text{He})$ Q value is -11.65 MeV in contrast to the Q value of -15.93 MeV for the (p, t) reaction.

Experimental and theoretical cross sections for the mass-25 ground states were also compared in terms of the enhancement factor ϵ by which the theoretical values must be scaled to match the experimental. Here ϵ was computed from Eq. (4.1) of Ref. 2 and a normalization factor D_0^2 of 22×10^4 $\text{MeV}^2 \text{fm}^3$ was included.³¹ The values of ϵ for $LSJ = 000$ and a bound-state well radius of 1.25 fm are included in Fig. 7. These values of ϵ indicate that the $(d_{3/2})^2$ configuration contributes much less to the cross section than do the $(d_{5/2})^2$ and $(2s_{1/2})^2$ configurations. Enhancement factors were also computed for the summed 000 + 202 DWUCK cross sections for the (p, t) ($\epsilon = 0.67$) and the $(p, {}^3\text{He})$ reactions. The configuration used was $(d_{5/2})^2$ with a bound-state well radius of 1.25 fm. Normalizing the $(p, {}^3\text{He})$ reaction was somewhat more complicated than for the (p, t) reaction. The $S=0, T=1$ and $S=1, T=0$ transfer processes have separate normalizations; for DWUCK, the normalization of the $S=0, T=1$ component of the $(p, {}^3\text{He})$ reaction is $\frac{1}{2}D_0^2$, where D_0^2 is the same as the (p, t)

normalization discussed above. Assuming that the $S=1, T=0$ strength is negligible, i.e., $D_1^2 = 0$, the enhancement factor for the ${}^{27}\text{Al}(p, {}^3\text{He}){}^{25}\text{Mg}$ ground-state transition was determined to be 0.50, less than that observed for the mirror (p, t) transition even though part of the reaction mechanism has not been accounted for. This suggests that the $S=1, T=0$ component of the $(p, {}^3\text{He})$ reaction contributes relatively little to the ground-state cross section.

Population of the first excited $J^\pi = \frac{1}{2}^+$ levels is of particular interest because the only permissible LSJ transfer for the (p, t) reaction is 202 while 202, 212, 213, and 413 are allowed for $(p, {}^3\text{He})$.

Two-neutron configurations including $(d_{5/2})^2$, $(d_{5/2}, s_{1/2})$, $(d_{5/2}, d_{3/2})$, and $(s_{1/2}, d_{3/2})$ were used in DWUCK calculations (with ZF parameter values) but all of the calculations yielded the characteristic $L=2$ maximum near 30° - inconsistent with the nearly structureless (p, t) data. Computations for $(p, {}^3\text{He})$ were carried out with the $(\pi d_{5/2}, \nu s_{1/2})$ configuration. An $L=2$ angular distribution computed with a coherent sum of equally weighted relative amplitudes of $S=0$ and $S=1$ transfers was indistinguishable from the calculation for $S=0$ alone shown in Fig. 2. While the characteristic $L=2$ maximum near 25° was reproduced by all the

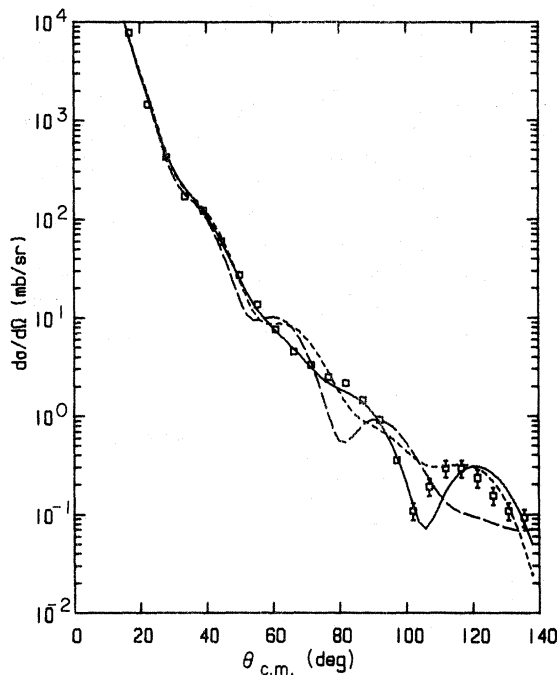


FIG. 5. Comparison of cross sections predicted by optical-model parameter sets ZF (solid), C (short dashes), and CR (long dashes) with experimental cross section (Ref. 21) for elastic scattering of 15-MeV ${}^3\text{He}$ from ${}^{24}\text{Mg}$.

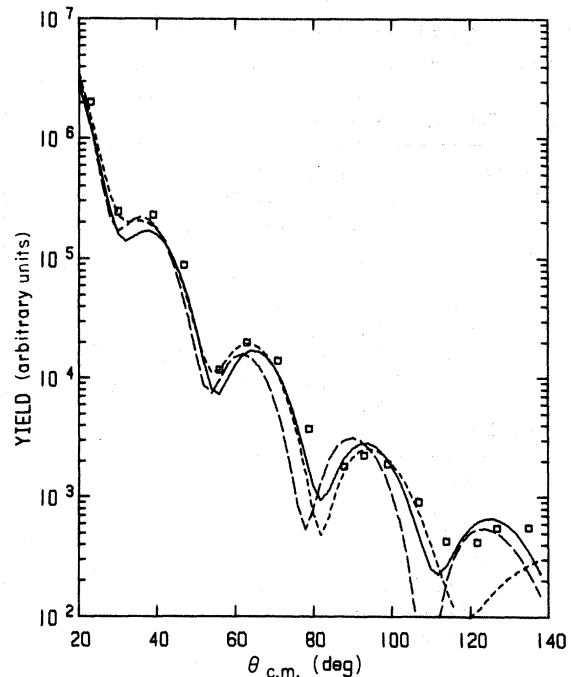


FIG. 6. Comparison of relative yields predicted by optical-model parameter sets GJ (solid), C (short dashes), and CR (long dashes) with experimental data (Ref. 23) for elastic scattering of 12-MeV tritons from ${}^{27}\text{Al}$. Fits obtained with sets GJS and GJD (not shown) were not significantly better than that obtained with set GJ.

calculations, none of the theoretical curves yielded a minimum near 90° .

Because of our inability to obtain a satisfactory description of the data with distorted-wave calculations, we also tried coupled-channel calculations for a (p, d) (d, t) two-step reaction process with the code CHUCK.³² The results arbitrarily normalized to the data appear in Fig. 2. These calculations considered the two-step process only; the single-step strength was set equal to zero. The reaction was assumed to proceed via pickup of a $d_{5/2}$ neutron leading to a 0^+ state in ^{26}Al followed by pickup of a $2s_{1/2}$ particle leading to the $\frac{1}{2}^+$ final state. Spectroscopic factors were computed assuming that the entire single-particle strength lay in these two transitions. Hence magnitudes of these calculations may be significantly overestimated. The calculated two-step magnitudes are larger than the experimental cross sections by a factor of 5 for the (p, t) reaction and a factor of 15 for the $(p, ^3\text{He})$ reaction. The coupled-channel calculation reproduced the shape of the triton angular distribution fairly well but did not fit the ^3He data.

For the $\frac{3}{2}^+$ level at 0.949 MeV the selection rules permit 202 and 404 (seniority-three) transitions. A sum of DWUCK cross sections for $(d_{5/2})^2$ fits the data (Fig. 2) quite well to 80° . The angular distribution for the $L=4$ component is almost struc-

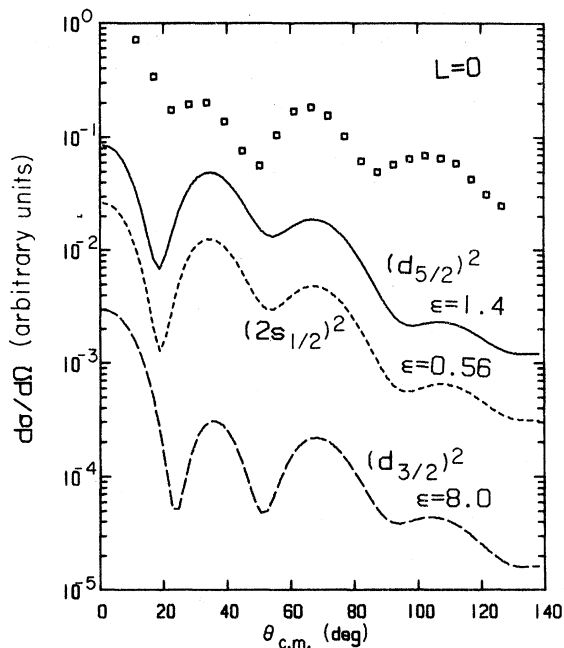


FIG. 7. Sensitivity of DWBA calculations to neutron-shell-model configuration. The theoretical curves have been computed for a bound-state radius of 1.25 fm and scaled arbitrarily.

tureless and decreases gradually with increasing angle. The shape of the angular distribution computed for $(d_{5/2}, d_{3/2})$ pickup is indistinguishable from the one shown. For the $(p, ^3\text{He})$ reaction to the corresponding level at 0.975 MeV LSJ transfers of 011, 211, 213, and 413 are also allowed. The DWUCK angular distribution for 211 had nearly the same shape as that for 202 but the cross section was an order of magnitude smaller. The fit shown in Fig. 2 for a 202 transfer was not improved by including the 011 component which was strong at angles forward of 20° and emphasized the minima.

The observed angular distributions (Fig. 2) for the $J^\pi = \frac{7}{2}^+$ levels at 1.61 MeV differ in that the (p, t) data do not indicate the sharp forward angle rise seen in the $(p, ^3\text{He})$ data and characteristic^{2,26} of $L=0$ transfer. For the (p, t) reaction LSJ transfers of 202, 404, and 606 are permissible while $L=0$ is forbidden. A fairly satisfactory fit was obtained with computations based on a $(d_{5/2})^2$ configuration and a sum of 202 and 404 DWUCK cross sections. The pickup process populating levels in the $A=25$ nuclei with $J = \frac{7}{2}$ and even parity necessarily requires breaking of at least two pairs (seniority three). The fit to the $(p, ^3\text{He})$ data involved the $(\pi d_{5/2}, \nu d_{5/2})$ configuration with a sum of DWUCK cross sections for LSJ transfers of 011, 202, and 404. A slightly greater admixture of 011 would provide an even better fit to the data at forward angles, but the positions of maxima and minima are not well reproduced.

Population of the $\frac{5}{2}^+$ levels at 1.81 and 1.96 MeV requires very little, if any, $L=0$ transfer. The experimental diffraction patterns shown in Fig. 3 seem to be out of phase too. The $\frac{9}{2}^+$ levels at 3.4 MeV are of interest because the (p, t) data (Fig. 3) indicate a prominent maximum near 40° while the $(p, ^3\text{He})$ data suggest a weak maximum near 40° and a strong rise toward forward angles. The

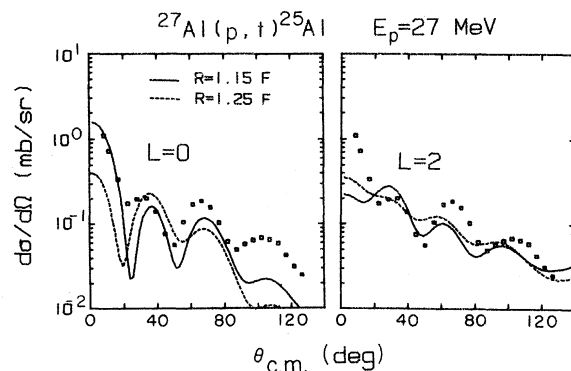


FIG. 8. Dependence of theoretical DWBA (DWUCK) angular distributions on the radius of the bound-state orbits for $L=0$ and $L=2$.

lowest permissible L transfer is 2 units and the strong rise at forward angles in the $(p, {}^3\text{He})$ data may be due to the presence of an unresolved $\frac{3}{2}^-$ level¹² at 3.40 MeV which could be reached through $L = 1$ transfer. The intensity of this level relative to that of the $\frac{3}{2}^+$ level is presumably small if comparison with the analogous, resolved levels at 3.08 and 3.44 MeV (Fig. 1) in ${}^{25}\text{Al}$ is valid. For still higher levels the energies of the outgoing triton and ${}^3\text{He}$ particles may be so low that direct interactions are dominated by compound-nucleus formation. Indeed very little diffraction structure is apparent in the angular distributions in Fig. 4.

E. Compound-Nucleus Computations

Theoretical expressions for cross sections for compound-nucleus reactions have been given by Hauser and Feshbach.³³ A simplified expression due to Eberhard *et al.*³⁴ has been utilized in the computer code CUMPND³⁵ and depends on only two parameters. One is σ_{res}^2 , the spin-distribution parameter in the residual nucleus. The other is $\rho' = 2\pi\Gamma_0\rho_0$, where ρ_0 is the density of levels with a spin of zero in the compound nucleus at the appropriate excitation energy and Γ_0 is the average width of these levels. The values used for σ_{res}^2 , Γ_0 , and ρ_0 are 10.24, 0.042 MeV, and 3.738×10^4 MeV⁻¹. These values provided a satisfactory empirical fit to the experimental cross section for population of a 5.22-MeV 3^+ level³⁶ observed here in the reaction ${}^{26}\text{Mg}(p, t){}^{24}\text{Mg}$. For this 3^+ level direct single-step excitation is forbidden. However, this fact does not imply that the *entire*

cross section is therefore due to compound-nucleus formation.

The results of our calculations with these parameter values are shown in Figs. 2-4. For each level up to 3.44 MeV excitation appropriate particle-transmission factors were computed with the code OPTIM¹⁶ from the optical potential and the ZF parameters of Table I. In Fig. 4 the higher levels in ${}^{25}\text{Al}$ are compared with a single compound-nucleus computation for a level at 5.00 MeV with spin $\frac{3}{2}$. The predicted angular distributions are smooth, symmetric about 90° , not very sensitive to spin or energy, and usually larger than the observed cross sections. The computations with the empirical parameter values listed above generally provide satisfactory fits for the weaker, featureless angular distributions. However, these parameter values are quite different from those deduced for lower excitation energies by Gilbert and Cameron.³⁷ A reasonable value of σ_{res}^2 is 4.0 according to the tabulation of Gilbert and Cameron. The cross-section calculations are quite sensitive to σ_{res}^2 as illustrated in Fig. 10. A calculation for an arbitrary intermediate value of $\sigma_{\text{res}}^2 = 7.0$ is also shown. The cross sections are inversely proportional to ρ' and hence ρ_0 . An expression³⁷ for ρ_0 yielded a value of 2.09×10^4 MeV⁻¹. Use of this value would increase all the compound-nucleus cross sections shown in Figs. 2-4 and 10 by nearly a factor of two. While the values obtained from the ${}^{26}\text{Mg}(p, t)$ reaction give results which seem reasonable, we have no other justification for their use. An incoherent sum of compound-nucleus reaction cross sections and DWBA cross sections

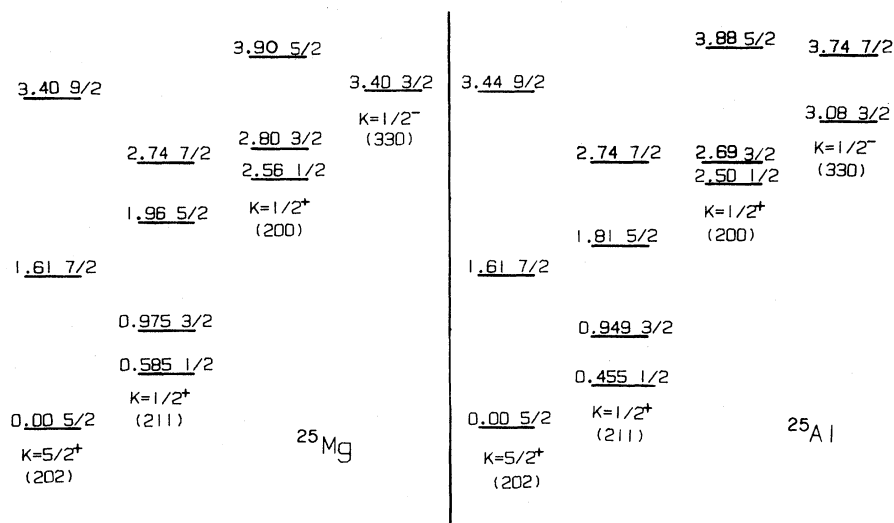


FIG. 9. Excited levels of ${}^{25}\text{Al}$ and ${}^{25}\text{Mg}$ grouped into rotational bands. The labels for each level indicate the energy and spin. The symbols below each band head indicate the K quantum number, parity, and asymptotic quantum numbers (N, n_z, Δ) in the Nilsson (Ref. 28) notation.

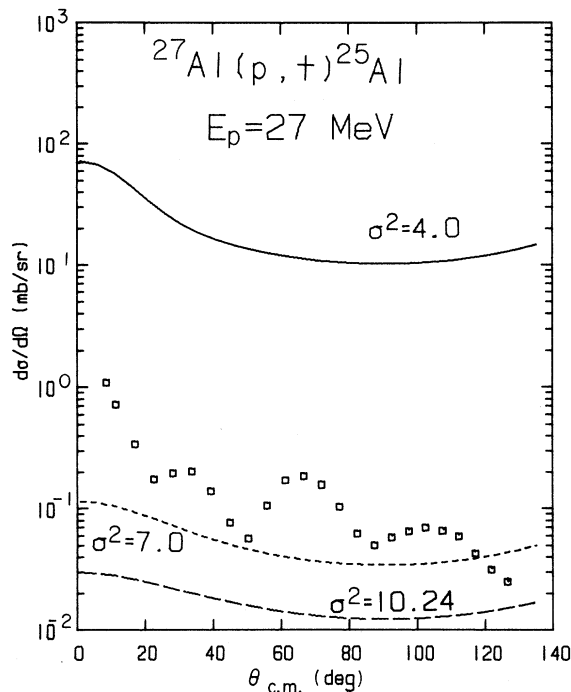


FIG. 10. Sensitivity of compound-nucleus cross sections to the spin-distribution parameter.

with appropriate weightings may fit most of the angular distributions observed here, although the contributions from the two-step processes may also be important.

However, the data for the weakly excited lowest spin- $\frac{1}{2}$ levels remain a puzzle. Both the two-step and compound processes could provide adequate fits to the data for the 0.455-MeV level in ^{25}Al . In contrast a reasonable fit to the structure at forward angles in the 0.585-MeV analog in ^{25}Mg is provided by the DWBA. However, none of the calculations fit the cusp observed near 90° . Possibly destructive interference between the two direct-interaction processes could produce such a minimum.

IV. CONCLUSIONS

The cross section for the excitation for a given state (Figs. 2 and 3) is very nearly the same for the (p, t) and $(p, {}^3\text{He})$ reaction with the exception of the ground state. For the ground state the (p, t) cross section is 2 to 3 times greater than the $(p, {}^3\text{He})$ cross section. Perhaps this observation can be correlated with the fact that the ground-state transitions are the only ones where the one-step-direct-reaction mechanism appears to dominate. It may be that differences between the direct (p, t) and $(p, {}^3\text{He})$ mechanisms can account for these differences in cross sections. The exact

nature of these differences is not clear. However, this situation can be contrasted with transitions to higher-lying states where the reaction mechanism is not certain but compound-nuclear processes seem important and do not depend on differences between the (p, t) and $(p, {}^3\text{He})$ direct-reaction mechanisms. In these cases (p, t) and $(p, {}^3\text{He})$ cross sections have nearly identical magnitudes.

The DWBA predictions for angular distributions for the first few levels excited by the (p, t) and $(p, {}^3\text{He})$ reactions on ^{27}Al fit the data quite well although the computations were somewhat sensitive to the optical-model-parameter values which determined the distorted waves. The calculations were insensitive to the choice of shell-model configuration for the picked-up particles but did depend on the radius of the neutron binding well. The predicted angular distribution shapes for ${}^3\text{He}$ were unchanged whether $S=0$ and $S=1$ contributions were calculated coherently or incoherently. Transitions which involved $L=0$ transfer retained their characteristic feature, the sharp rise at forward angles, even though appreciable L mixing may have been present.

The compound-nucleus calculations reproduced satisfactorily the angular distribution shapes for weak, higher excited levels, but the predicted cross sections were consistently too large even when parameter values used successfully for analysis of $^{26}\text{Mg}(p, t)$ data were employed. The computed cross sections were quite sensitive to σ_{res}^2 , the spin distribution parameter for the residual nucleus.

Neither the DWBA nor the compound-nucleus computations were able to account consistently for the dissimilar angular distributions of the $\frac{1}{2}^+$ levels near 0.5 MeV excitation. A two-step (p, d) (d, t) computation also failed to reproduce both angular distributions simultaneously, but the large predicted strength suggests two-step processes may be important here.

Finally, the (p, t) data indicated the presence of three new levels in ^{25}Al . The relatively flat angular distributions, which are indicative of compound-nucleus formation or possibly multiple unresolved levels, did not permit extraction of the transferred orbital angular momentum L . It was also not possible to obtain quantitative information on the ground-state wave function for ^{27}Al .

ACKNOWLEDGMENTS

We thank B. Briggs for assistance in data reduction and Professor E. S. Rost and Professor P. D. Kunz for discussions of transfer reactions. We are also indebted to Dr. L. Parish for providing us with a copy of his program for doing Hauser-Feshbach calculations.

- *Work supported in part by the U. S. Atomic Energy Commission.
- † On leave from The Pennsylvania State University, University Park, Pennsylvania 16802.
- ¹H. W. Baer, J. J. Kraushaar, C. E. Moss, N. S. P. King, and R. E. L. Green, *Phys. Rev. Letters* **25**, 1035 (1970).
- ²H. W. Baer, J. J. Kraushaar, C. E. Moss, N. S. P. King, R. E. L. Green, P. D. Kunz, and E. Rost, *Ann. Phys. (N.Y.)* (to be published).
- ³A. E. Litherland, H. McManus, E. B. Paul, D. A. Bromley, and H. E. Gove, *Can. J. Phys.* **36**, 378 (1958).
- ⁴J. C. Hardy, H. Brunnader, and J. Cerny, *Phys. Rev. Letters* **22**, 1439 (1969).
- ⁵W. Bohne, H. Fuchs, K. Grabisch, M. Hagen, H. Homeyer, U. Janetzki, H. Lettau, K. H. Maier, H. Morgenstern, P. Pietrzyk, G. Röscher, and J. A. Scheer, *Nucl. Phys.* **A131**, 273 (1969).
- ⁶G. M. Reynolds, J. R. Maxwell, and N. M. Hintz, *Bull. Am. Phys. Soc.* **10**, 439 (1965).
- ⁷R. E. Brown, C. G. Hoot, N. M. Hintz, J. R. Maxwell, and A. Scott, *Bull. Am. Phys. Soc.* **11**, 316 (1966).
- ⁸J. C. Hardy and D. J. Skryme, *Bull. Am. Phys. Soc.* **11**, 627 (1966); in *Isobaric Spin in Nuclear Physics*, edited by J. D. Fox and D. Robson (Academic, New York, 1966), p. 701.
- ⁹I. S. Towner and J. C. Hardy, *Adv. Phys.* **18**, 401 (1969).
- ¹⁰R. Graetzer, J. J. Kraushaar, and J. R. Shepard, *Bull. Am. Phys. Soc.* **17**, 90 (1972).
- ¹¹A. H. Wapstra and N. B. Gove, *Nucl. Data* **A9**, 265 (1971).
- ¹²P. M. Endt and C. Van der Leun, *Nucl. Phys.* **A105**, 1 (1967).
- ¹³P. Ingall, University of Colorado, private communication.
- ¹⁴C. P. Browne, private communication; *Bull. Am. Phys. Soc.* **17**, 532 (1972).
- ¹⁵J. R. Duray *et al.*, quoted in Ref. 14.
- ¹⁶D. H. Zurstadt, University of Colorado, private communication.
- ¹⁷N. K. Glendenning, *Phys. Rev.* **137**, B102 (1965).
- ¹⁸P. D. Kunz, University of Colorado (unpublished).
- ¹⁹G. R. Satchler, *Nucl. Phys.* **A92**, 273 (1967).
- ²⁰P. P. Urone, L. W. Put, H. H. Chang, and B. W. Ridley, *Nucl. Phys.* **A163**, 225 (1971).
- ²¹R. W. Zürmühle and C. M. Fou, *Nucl. Phys.* **A129**, 502 (1969).
- ²²R. A. Morrison, *Nucl. Phys.* **A140**, 97 (1970).
- ²³R. N. Glover and A. D. W. Jones, *Nucl. Phys.* **81**, 268 (1966).
- ²⁴H. H. Chang, University of Colorado, private communication.
- ²⁵H. H. Chang and B. W. Ridley, University of Colorado Nuclear Physics Laboratory Technical Progress Report No. COO-535-653 (unpublished), p. 55.
- ²⁶J. R. Shepard, J. J. Kraushaar, and R. Graetzer, to be published.
- ²⁷B. E. Chi, *Nucl. Phys.* **83**, 97 (1966).
- ²⁸B. R. Mottelson and S. G. Nilsson, *Kgl. Danske Videnskab. Selskab, Mat-Fys. Skrifter* **1**, No. 8 (1959).
- ²⁹H. Röpke, V. Glattes, and G. Hammel, *Nucl. Phys.* **A156**, 477 (1970).
- ³⁰N. J. A. DeVoigt, P. W. M. Glaudemans, J. DeBoer, and B. H. Wildenthal, *Nucl. Phys.* **A186**, 365 (1972).
- ³¹J. R. Ball, R. L. Auble, and P. G. Roos, *Phys. Rev. C* **4**, 196 (1971).
- ³²P. D. Kunz and E. Rost, *Bull. Am. Phys. Soc.* **17**, 509 (1972).
- ³³W. Hauser and H. Feshbach, *Phys. Rev.* **87**, 366 (1952).
- ³⁴K. A. Eberhard, P. Von Brentano, M. Böhning, and R. O. Stephen, *Nucl. Phys.* **A125**, 673 (1969).
- ³⁵L. Parish, University of Minnesota (unpublished).
- ³⁶K. W. Kemper and A. W. Obst, *Phys. Rev. C* **6**, 672 (1972).
- ³⁷A. Gilbert and A. G. W. Cameron, *Can. J. Phys.* **43**, 1446 (1965).